Chapter 4

Exposure to a commercial combination of chlorpyrifos 50 % + cypermethrin 5 % deranged the expression pattern of crucial signalling molecules that facilitate the patterning of neural tube in domestic chick

4.1. INTRODUCTION

The development of an embryo encompasses a complex process, which has always kept the man spell bounded since the beginning of history. Certain fundamental questions were unearthed through the usage of several animal model systems such as Drosophila, *C. elegans*, *Xenopus*, chick and mouse. These models have offered several valuable insights in studying the developmental mechanisms up to different extents. Of these, the chicken was one of the first vertebrate model to be used for developmental investigations such as dorso-ventral patterning (Davey, 2018), neurulation (Kantarcioglu et al., 2018; Schoenwolf, 2018), and left–right asymmetry (Monsoro-Burq and Levin, 2018). It remains as a popular model for research over two millennia for understanding cellular and molecular mechanism of vertebrate development. Moreover, embryonic stages and genome of chick have considerable homology with human, making it more attractive to study developmental processes like intracellular communication, cell migration and morphogenetic movements (Stern, 2005; 2018). The advantages of the chick are numerous, making it almost an ideal model for studying neurobehavioral teratogenicity and associated mechanisms (Wormser et al., 2005; Abdul-Ghani et al., 2012).

Wilson (1973) suggested that early developmental stages of an embryo are more susceptible to various maternal and environmental stressors, in the whole of their life cycle (Figure 4.1). The factors reported to cause congenital abnormalities in the embryos are temperature (Rashid et al., 2017), hypoxic condition (Webster and Abela, 2007), UV rays (Williams and Fletcher, 2010; Megaw et al., 2017; Botyar and Khoramroudi, 2018), free radicals (Loeken, 2004), and pesticides (García, 2003; Rappazzo et al., 2016; Kalliora et al., 2018; Ramakrishnan and Jayaraman, 2019). Out of these man-made chemicals, pesticides are of a special concern due to

its widespread usage in day to day life. A real-life example of thalidomide confirmed how vulnerable an embryo is towards its usage resulting into severe congenital defects in thousands of children. In addition, several reports have come forward, proving detrimental effects of pesticides on humans and their role in causing congenital defects. Additionally, the teratogenic potential of pesticides has also been emphasised widely by the experiments using avian and rodent model systems (Madu, 2015; Yu et al., 2017; Abbas et al., 2018; Salvaggio et al., 2018).

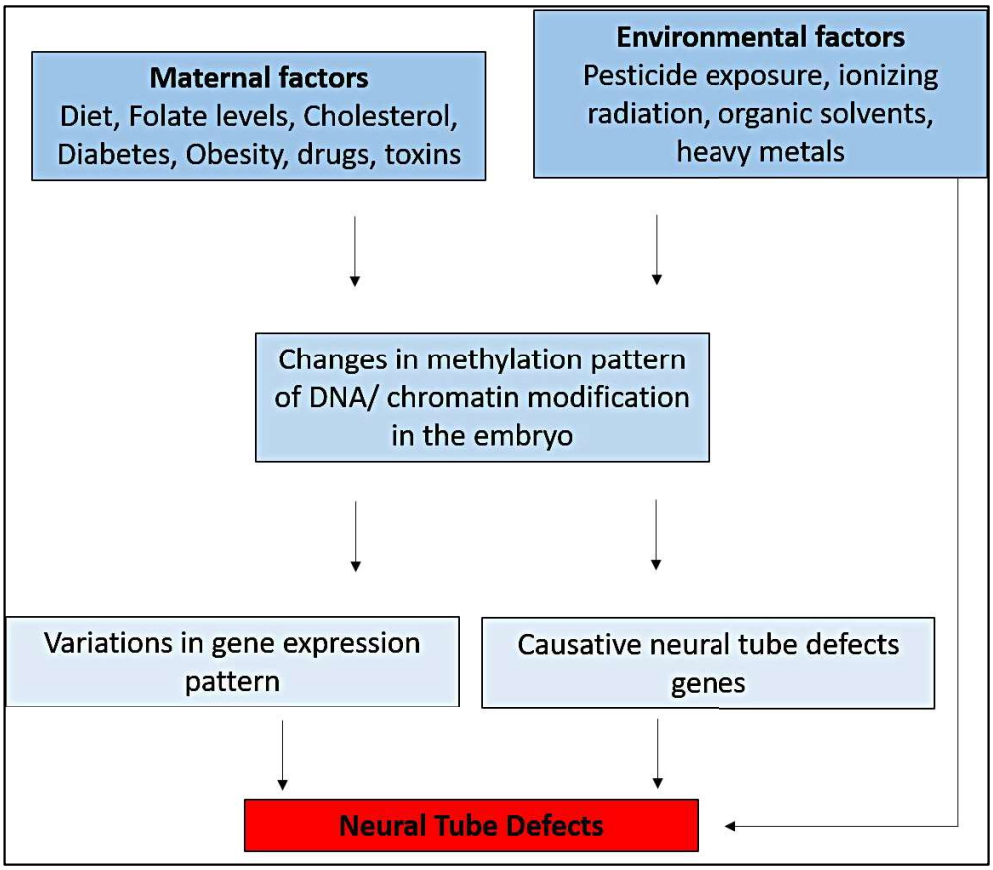

Figure 4.1: A pictorial representation of the factors causing neural tube defects.

Reports are available for increasing evidences of a variety of pesticide exposure resulting into congenital birth defects pertaining to neural tube formation and development (Wang et al., 2017). The Neural tube defects (NTDs) are more common than any other congenital defects, affecting over 300,000 births every year (NCBDDD, 2012). There are several factors causing defects in the development of central nervous system (Figure 4.1). These anomalies relate to the disturbances in normal growth and development of the brain, spine and other essential craniofacial structures. Against this backdrop our lab has conducted a series of teratological screening of one of the most widely used insecticide combination (Chlorpyrifos 50 % +

Cypermethrin 5 %) in chick. The result showed widespread malformations in the hatchlings of combination insecticide (Ci) treated eggs like distorted cephalization, anophthalmia, wry neck, craniorachischisis, diprosopus and ventral body wall defects (Uggini et al., 2012; Uggini and Suresh, 2013; Sharma et al., 2018). Moreover, these investigations have inferences towards the derailed molecular signalling during the early embryonic development that led to neural tube defects. Therefore, to gain insight on the Ci interventions over the signalling pathways, it was well-thought-out to monitor the early developmental processes (herein the neural tube formation) in the avian embryo which might possibly give evidences to how these deformities were caused. Therefore, a concise briefing of the early developmental events that might have been targeted by the Ci are discussed below:

4.2. NEURULATION

The early embryonic development starts with the fertilization and proceeds further as morphogenesis that includes blastula formation, gastrulation, histogenesis and lastly organogenesis (Gilbert, 2003). The early cellular movements occurring during these stages of development are intricate, intertwined and follow a stringent spatial extension and temporal expression pattern. Amongst all the stages that a fertilized egg undergoes, gastrulation epitomises the primary step in breaking its disc shaped and single layered symmetry. This progression of the embryo towards gastrula phase, makes the embryo asymmetric, required for forming proximal-distal and dorso-ventral axes (Castro-e-Silva and Bernardes, 2005). Accordingly, these cellular movements allow the cells to intercommunicate with their surroundings and pave the way for neurulation followed by organogenesis.

Neurulation encompasses the development of a flat neural plate that subsequently converts into a hollow neural tube. The embryo during this conversion is referred to be in neurula stage. The formation of neural tube is complex and regulated by many genetic and environmental factors. In chicken embryo, the notochord induces the ectoderm to form a thick neural plate which eventually converges, folds and fuses at the dorsal midline to develop into a neural tube (Figure 4.2). Subsequently, with the help of intrinsic processes such as cell patterning, proliferation and migration the primary lobes are formed on the anterior end of the neural tube (Figure 4.3), which later develop into complex structures of the brain (Wilson et al., 2001; Schoenwolf, 2018).

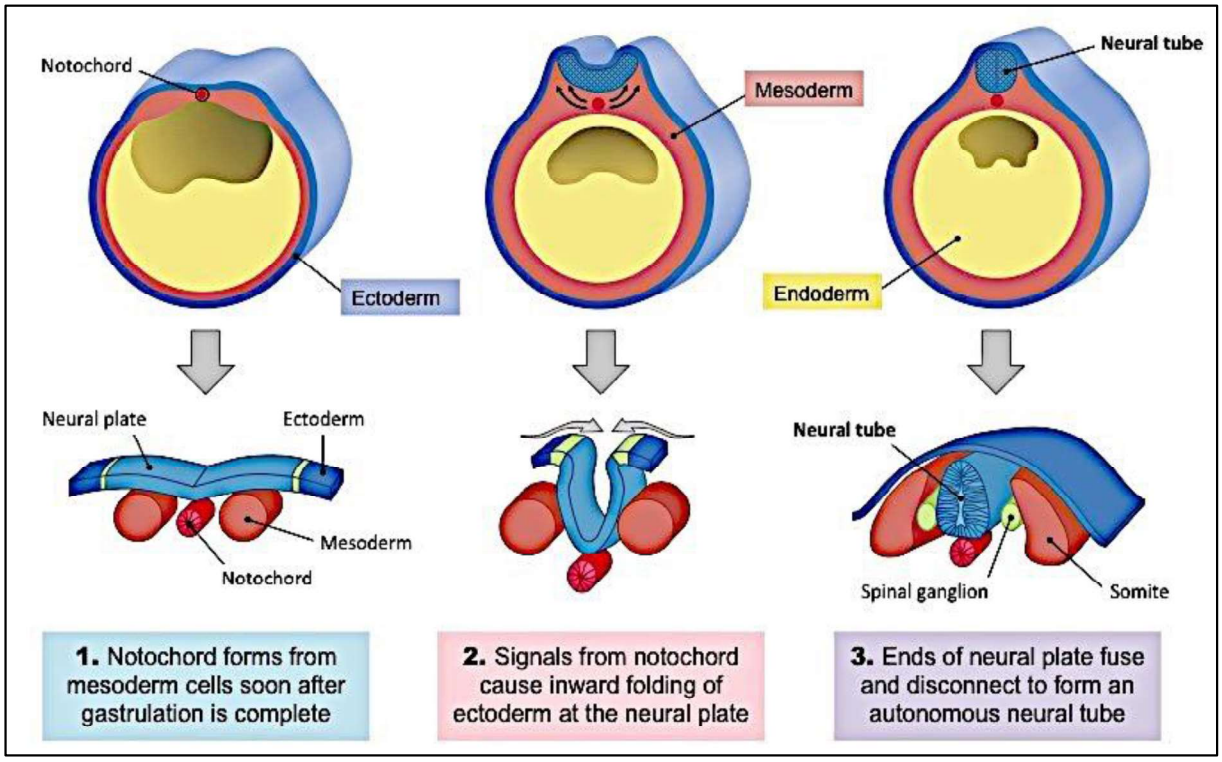

Figure 4.2: Schematic representation of neural tube formation from an ectodermal plate in amniotes. Source: http://ib.bioninja.com.au

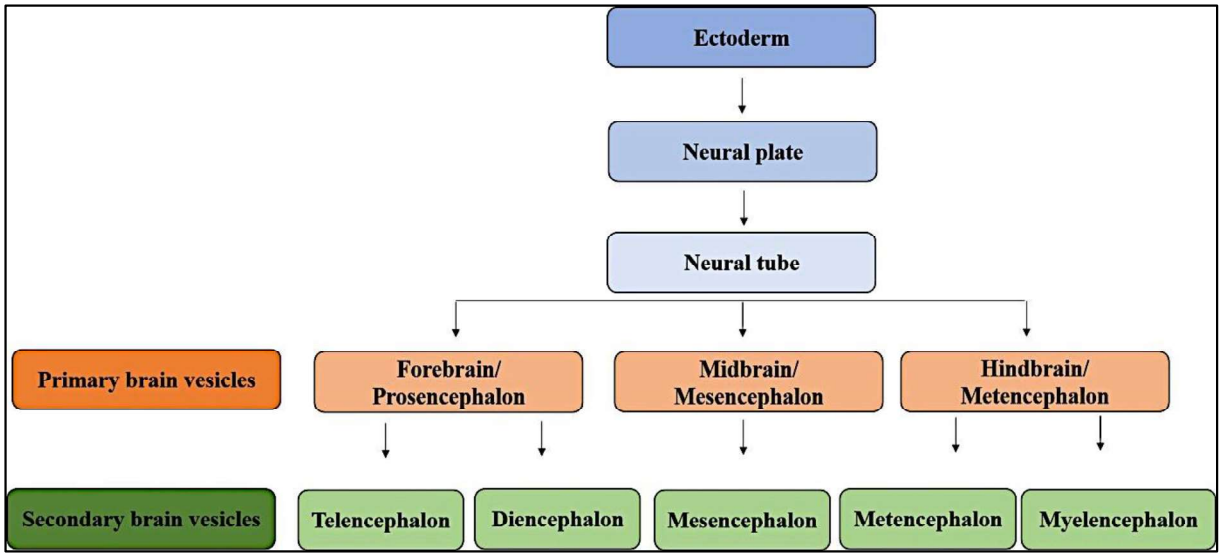

Figure 4.3: Flowchart depicting formation of brain vesicles from a single layered ectoderm. Adapted from: Gilbert, 2003

4.3. NEURAL TUBE CLOSURE

One of the most critical events occurring in the development of central nervous system is the closure of neural tube. Any failure in the closure process results in the neural tube defects and is one of the most commonly occurring congenital anomalies. These defects leave loopholes in the protection of the spinal cord and the brain, leaving them vulnerable to damage. Due to these failures, the organism may fall prey to any damage leading to paralysis or even death. Moreover, these disorders arise at the early stages of development causing hitches in the survival of the organism and damages of variable severity. These devastating conditions affect thousands of families each year (NCBDDD, 2012). The main NTDs are anencephaly, encephalocele and spina bifida. Numerous investigations on different vertebrate embryos have suggested defects in neurulation process, occurring due to maternal exposure to environmental chemicals including pesticides (Podgórski et al., 2017; Nilolopoulou et al., 2017; Alexander et al., 2018).

4.4. NEURAL CREST CELL MOVEMENT

The neural crest (NC) cells are the temporary group of cells that delaminate from the neural plate after the fusion of neural folds. These cells pattern along the dorso-ventral and antero-posterior axes to give rise to neurons, glia and facial skeleton. A series of gene regulatory networks influences the development of neural crest cells and their interaction with mesenchymal cells. Moreover, their migration involves the loss of calcium dependent signalling molecules such as E-cadherins, N-cadherins and cell-to-cell adhesion molecules to give rise to various facial derivatives along the anterior-posterior axis of the embryo. Ahlgren and Bronner-Fraser (1999), have differentiated the types of neural crest cells depending on the structures they give rise to, along the rostro-caudal axis of the embryo:

Crest cell type	Fate
Cranial neural crest cells (CNCC)	Connective tissue and skeletal contributions to the face, Schwann cells, ciliary and cranial sensory ganglia
Vagal neural crest cells (VNCC)	Enteric nervous system
Trunk neural crest cells (TNCC)	Melanocytes, sensory and sympathetic ganglia, Schwann cells, adrenomedullary cells
Lumbo-sacral neural crest cells (LNCC)	Enteric nervous system

4.5. CHONDROGENESIS

Among the types of neural crest cells mentioned above, the cranial neural crest cells give rise to the frontonasal skeleton that forms the maxillary and mandibular bones. In the embryonic development the mesenchymal cells give rise to the endoskeleton made up of cartilage that in due course differentiates into chondrocytes and begins to form extracellular matrix. The cartilage is then gradually ossified and the phenomenon is referred as chondrogenesis. The craniofacial structures are a result of the activities of cranial neural crest cells and mesodermal derivatives along with ossification (Ahlgren and Bronner-Fraser, 1999). CNCs undergo dorso-ventral patterning to form the neural tube and differentiate into chondroprogenitor cells forming the neuro-cranium in the tetrapods. Several reports have confirmed their interactions with the mesenchymal derivatives obligatory for the facial development (McBratney-Owen et al., 2008; Wada et al., 2011; McCarthy et al., 2016). Therefore, any defect in patterning, proliferation, migration or differentiation of the cranial neural crest cell population would contribute to the craniofacial malformations (Wilkie and Morriss-Kay, 2001; Dixon et al., 2006).

4.6. THE EARLY GENE EXPRESSION

The key processes in craniofacial development include cranial neural crest development (e.g., induction, specification, delamination and migration), morphogenesis (e.g., patterning, growth, and fusion of the facial primordia) and histogenesis (e.g., tissue differentiation) (Fish, 2016). These morphogenetic events are suggested to be tightly regulated by several gene products or genetic factors which coordinate the craniofacial formation. These regulators include many signalling molecules that orchestrate different pathways *viz*. SHH, FGFs, BMPs, and WNTs which further regulate the complex cellular processes such as cell adhesion, migration, proliferation and apoptosis (Alexander et al., 2011; Richtsmeier and Flaherty, 2013; Schock et al., 2016; Suzuki et al., 2016). For instance, the Fibroblast Growth Factor 8 (FGF8) expression has been observed in neuro-mesodermal population and its derivatives, where it interacts with other signalling pathways (Diez del Corral and Morales, 2017). Moreover, Sonic hedgehog (SHH) has been shown to be expressed by the notochord and floor plate in the developing spinal cord. Depending on the time of embryonic development and location in the embryo, its expression becomes critical in deciding the fate of cell for proliferation or survival (Yang and Ornitz, et al., 2019).

4.7. OBJECTIVE OF THE STUDY

The craniofacial anomalies were observed in the chicken hatchlings which failed to reach the developmental milestones including neural tube closure and migration of neural crest cells due to the exposure of combination insecticide. However, the molecular mechanism leading to the Ci toxicity remained elusive.

In order to deduce the effect of Ci, the present study focused on the signalling molecules that facilitates the sequential development of craniofacial structures in the chick embryos of three different developmental stages namely Hamburger and Hamilton (HH) stage 13, 24 and 36 (corresponding to days 2, 4 and 10 of embryonic development) (Hamburger and Hamilton, 1951). The day 2 embryo is characterized by the presence of primary optic vesicles and well-established optic stalk along with a distinct telencephalon and forebrain covered with head fold of amnion. However, distinct eye pigmentation and enlargement of head structures can be observed by day 4. On day 10, primary calcification of the body begins which extends towards the remaining cartilaginous area until the hatching (Sawad et al., 2009). The selected stages, therefore, helped in understanding the levels of few key molecular signals involved in neural tube patterning and endochondral ossification during early stages of chick embryonic development upon *in ovo* exposure of combination insecticide.

4.8. MATERIALS AND METHODS

4.8.1. Toxicant

The test article formulation constituted of a mixture of chlorpyrifos (50 %) and cypermethrin (5 %). It is commercially retailed as Anaconda 505^{TM} and manufactured by AIMCO Pesticides Pvt. Ltd., Mumbai, India.

4.8.2. Test system

Fertilized eggs of Rhode Island Red (*Gallus domesticus*) breed of domestic chicken were used in the study and were procured from the Intensive Poultry Development Unit, Vadodara, India. The conduct of experimental protocols was in full compliance with the guidelines of Drugs and Cosmetics Rules 1945, Appendix-III animal care standard and were approved by the institutional animal ethics committee (Protocol number: IAEC 84/08/2014-2) in accordance with the norms of the committee for the purpose of control and supervision of experiments on animals (CPCSEA), India

4.8.3. Experimental design

The eggs were divided at random into control and treatment groups after being properly disinfected with 0.5 % povidone iodine solution. With the help candling method, air space was marked with a pencil and later the eggshell was punctured on day "0" of incubation, with a fine needle (Blankenship et al., 2003). Olive oil (Figaro, India) was injected in the control groups whereas the treatment group was administered with sub-lethal dose (0.05 µg per egg) of pesticide solution with olive oil as vehicle. Previous work from the lab aided to choose the ideal dosage for the study (Uggini et al., 2012). The whole procedure was strictly carried out in sterile condition in the laminar air hood to avoid any contamination. All the eggs were kept with their broad ends facing upwards in an automated incubator (Scientific equipment works, New Delhi) at a temperature of 37.5 °C ± 0.5 and relative humidity of 70 – 75 %. The eggs were automatically rotated every hour and were checked for mortality every two days till the day of sample collection.

4.8.4. Embryo collection

The eggs were cracked opened with the help of a scalpel and subsequently checked for the Hamilton-Hamburger (HH) stages of chick development. The embryos that had reached HH stage 13 (day 2), HH stage 24 (day 4) and HH stage 36 (day 10) were only collected for the study.

4.8.5. Rate of mortality and malformations

The embryos were collected at day 2, day 4 and day 10 of incubation. The rate of mortality and malformations was recorded on all three stages. In day 10 embryos, the size of the head was also measured with the help of Vernier calliper (Mitutoyo, Japan) The experiment was performed thrice with 30 eggs in each group (control and treatment) each time.

4.8.6. Real time RT-PCR

The chick embryos were isolated (n=10) and rinsed with cold PBS. Head region was specifically dissected out from control and treatment groups and was homogenized using TRIzol reagent (Applied Biosystems, USA) for total RNA isolation. cDNA was synthesized using one step cDNA synthesis kit procured from Applied Biosystems, USA. As per the recommended protocol, only 1 microgram of total RNA was used for cDNA synthesis. The primer sequences used in the study were obtained from NCBI and are listed as follows: *SHH, CASPASE 3, WNT5A, FGFG8, WNT7A, L1CAM, BMP7, GLI3, PCNA, WNT1, HOX10A,*

PAX6, HOX11A, CDH1, CDH2, FGF2, BMP2, GLI2, SOX9, RUNX2, DLX5 and *COL10A1*. Quantitative RT-PCR was performed using Lightcycler96 (Roche Diagnostics, Switzerland). The following program was set for the reaction to be carried out: denaturation for 100 s at 95 °C followed by 42 cycles of amplification (10 s at 95°C, 30 s at 60 °C, 30 s at 72 °C). To confirm the specific product formed by the reaction mixture, melt curve analysis and gel electrophoresis were performed. After the analysis, fold change was calculated and represented as $2^{-\Delta\Delta Cq}$ according to Livak and Schmittgen (2001). 18SrRNA was used as an endogenous control.

4.8.7. Protein expression analysis

Tissues (only head region) were collected on day 2, 4 and 10 from both control and treatment group (n=10). These test samples were homogenised and pooled in Tris-SDS lysis buffer with protease inhibitor (Sigma-Aldrich, USA). 10 % homogenates were assayed for total protein content by Bradford method (1976). Equal amount of total protein was loaded and separated by SDS-PAGE on 10 % gels. Protein was transferred onto nitrocellulose membrane by semi-dry transfer at 100 mA for 30 min. The membrane was probed separately with antibodies against 0.1 µg/ml of anti-SHH IgG Mouse, anti-Cl. CASPASE 3 IgG Rabbit, anti-PAX6 IgG Mouse, anti-E-Cadherin IgG Mouse, anti-N-Cadherin IgG Mouse, anti-BMP2 IgG Mouse and anti-β-Actin IgG Mouse. The blot was developed by ALP, BCIP-NBT system (Sigma-Aldrich, USA).

4.8.8. Hydroxyproline estimation

The tissues from the cranial region (n=10) of day 10 experimental groups (control and Ci treated) were excised to estimate the hydroxyproline content, as described by Edwards and O'Brien (1980). The samples were first dried and then acid hydrolysed at 120°C in a pressure vessel for 2-4 hours. Upon completion of hydrolysis, hydrolysates and standards tubes were kept in oven at 60 °C for 8 hours for complete evaporation of water. The homogenates and standards were added to 1.5 mL tubes, along with the same volume of citric/acetate buffer of pH 6.0 (citric acid, sodium acetate, sodium hydroxide, glacial acetic acid, n-propanol) and chloramine-T solution (chloramine-T dissolved in Milli-Q water). The tubes were incubated for 20 min at room temperature and Ehrlich's solution (p-dimethyl-amino benzaldehyde, perchloric acid and n-propanol) was added to the tubes which were then incubated at 60 °C for 15 min. The absorbance of the reaction product was read at 550 nm. The amount of hydroxyproline in each sample was calculated using regression curve of standard graph.

4.8.9. Alcian blue and Alizarin red staining

Ten embryos were collected at day 10 for visualizing the skeletal impairments. The embryos from both the experimental groups were fixed in 4 % paraformaldehyde and later washed in PBS for 2-3 days. These samples were stained for 6 hours in dark condition at room temperature with a filtered (0.1 %) Alcian blue and (0.1 %) Alizarin red solution (in 30 % acetic acid and 70 % ethanol) and dehydrated in 95 % ethanol for an hour. The tissues were then washed under tap water for 2 hours and afterwards transferred to 1 % potassium hydroxide solution for 2 hours. These samples were destained in a graded sequence of glycerol and potassium hydroxide and finally stored in 100 % glycerol at 4 °C (Depew, 2008).

4.8.10. Histological studies

The embryos were isolated, rinsed in PBS. Later the cranial region was excised and then fixed in 10% neutral buffered formalin. The tissue was further processed and paraffin wax blocks of the tissue samples were prepared. Longitudinal sections of 5µm thickness of head region of day 10 embryos were taken and stained with Harris haematoxylin and eosin. The histological details of the tissues on the slide were visualized using Leica DM2500 Microscope and pictures were captured using EC3 Camera (utilizing LAS EZ software).

4.8.11. Statistical analysis

The data for mortality and malformations were analysed for statistical significance by Mann-Whitney U Test. The rest of the data were analysed by two-tailed Student's t-test using Prism v5.03 (GraphPad Software Inc., USA). Values were expressed as mean ± standard error of mean. p value less than or equal to 0.05 was considered as statistically significant.

4.9. RESULTS

4.9.1. Day 2

The control group (Figure 4.4A) on day 2 (HH stage 12) showed characteristic features of the left profile of the head like clearly demarcated telencephalon, well established optic vesicles and optic stalk as well as S-shaped heart. On the other hand, the pesticide treated embryos showed significant rate of mortality (Table 4.1). Additionally, the treatment group of embryos exhibited many overt signs of toxicity with respect to craniofacial development. The rate of occurrence of malformations was significantly higher in the treated groups (Table 4.2). The signs of aberrations such as underdeveloped heart (Figure 4.4B), reduction in size of the whole

embryo (Figure 4.5A), absence of eye stalk (Figure 4.5B), underdeveloped telencephalon (Figure 4.5C), defect in closure of neural tube (Figure 4.5D) and distorted cephalisation (Figure 4.5E). In addition, an interesting feature of wavy neutral tube, was noticed in the treatment groups (Figure 4.4B). In order to validate the morphological observations, certain signalling molecules were studied at gene and protein expression levels. The relative mRNA expression levels of *SHH, WNT7A, L1CAM, BMP7, GLI3, HOX10A, HOX11A, WNT5A, WNT1, CDH1, CDH2, PCNA* and *PAX6* were found to be significantly lowered in the treatment group on day 2 when compared to the controls (Figure 4.6; Table 4.5). However, the expression levels of *CASPASE 3* and *FGF8* were found to be upregulated (Figure 4.6; Table 4.5). Immunoblot analysis revealed reduced expressions of SHH, PAX6, E-Cadherin and N-Cadherin in the treated embryos on day 2 compared to the control embryos (Figure 4.7). All the representative markers used in the blots were simultaneously checked for spot densitometry, revealing an observable and noteworthy reduction with respect to control group (Table 4.3).

4.9.2. Day 4

In the day 4 (HH stage 24) treated embryos, there was significant rate of mortality (Table 4.1) as well as an increased rate of occurrence of malformations (Table 4.2). The control group showed normal development with distinct optic cup, eye pigmentation, limb buds and allantois (Figure 4.8A). Visual examination of treated embryos showed defects like anophthalmia, reduced allantois and stunted growth (Figure 4.8B). Moreover, brain lobes like telencephalon, mesencephalon and metencephalon were reduced in size as compared to control embryos (Figure 4.8B).

To look into the molecular mechanism behind these malformations observed in treated embryos, few key signalling molecules involved in normal development of chick embryo were investigated at gene and protein level. Relative mRNA expression levels in day 4 treated embryos exhibited remarkable downregulation of *SHH, WNT5A, L1CAM, GLI3, WNT1, HOX10A, HOX11A, PAX6, CDH1* and *CDH2* expressions. While the *PCNA* and *WNT7A* levels were conspicuously reduced ($p \leq 0.01$) in the treated embryos, the change in expression levels of *BMP7* was found statistically insignificant. On the contrary, *CASPASE 3* and *FGF8* revealed an increased expression (Figure 4.9; Table 4.6). Western blot results for CASPASE 3 and SHH were in agreement with their respective gene expression levels (Figure 4.10; Table 4.3).

4.9.3. Day 10

Significant increase in the rate of mortality (Table 4.1) as well as occurrence of malformations (Table 4.2) was noted in treatment group of day 10 (HH stage 36) embryo. The control set of embryos (Figure 4.11A) on day 10 showed usual development of head, well defined beak and visceral organ. The embryos from treatment group showed exposed brain (Figure 4.11B), unilateral anophthalmia and phocomelia (Figure 4.11C), bilateral anophthalmia (Figure 4.11D), absence of beak (Figure 4.11E) and exposed visceral organs (Figure 4.11B-E). Also, morphometric analysis was carried out on the embryos using a Vernier calliper that revealed a significant reduction in the size of the head in treatment groups (Table 4.4).

Further, growth factors and few downstream mediators involved in governing or regulating the growth and patterning of chick embryo were found to show significant changes. The Ci dosed embryos showed a considerably diminished expression of *SOX9, COL10A1, BMP7, WNT5A* and *RUNX2* whereas *CASPASE 3* and *FGF8* mRNA levels were found to show an amplified expression. No noticeable changes were seen in case of *DLX5, FGF2, GLI3* and *GLI2* gene expression (Figure 4.12; Table 4.7). The treated samples from day 10 embryos showed reduced expressions of *SHH* and *BMP2* at both gene and protein levels (Figure 4.12, 4.17). The test group showed relatively subsided band intensities compared to control group (Table 4.3).

The extent of damage caused by the pesticide load in the tissue architecture was studied by differential staining in day 10 chick embryos by using haematoxylin and eosin. The control embryos on day 10 showed properly developed frontonasal structures including the beak. The frontal, prefrontal bones along with ear fossa were clearly demarcated. Whereas in the treatment group, the embryo showed maldeveloped facial structures. Moreover, a reduction in the size of the cranial vault was also noted. The histological picture of day 10 treated embryos showed no beak development and the ear fossa was found to be absent (Figure 4.13; 4.14).

Additionally, the extent of chondrogenesis was checked through differential staining of cranial region in day 10 chick embryos by Alcian blue (stains cartilage) and Alizarin red (stains bone). It was evident from the results that there is a marked reduction in endochondral ossification in the cranial region of the Ci treated embryos (Figure 4.15A, B). Alizarin red stained bones of lower jaw exhibited an incomplete fusion as well as partial ossification in treated embryos as opposed to the control ones (Figure 4.15A, B). Moreover, upon removal of eyeball from

embryos, the interorbital sinus in treated embryos illustrated hampered chondrogenesis in contrast to embryos of the control group. The extent of ossification of pre-maxilla and maxilla bones (involved in beak formation) was also reduced in treated embryos (Figure 4.15 A, B). The results obtained by Alcian blue- Alizarin red staining was further reaffirmed by biochemical estimation of hydroxyproline. A sharp drop was observed in hydroxyproline content in treated groups as compared to that of control one in day 10 embryos (Figure 4.16).

4.10. DISCUSSION

The ominous danger of insecticide intoxication during development is extremely worrisome since a brief exposure during the critical window of embryonic development can cause highly distressing morphological and anatomical anomalies. We tried to understand the possible alterations in the signalling pathways during the early embryogenesis which might have led to the observed craniofacial dysmorphism provoked by combination insecticide exposure. Much of the embryonic dysmorphs observed here could be attributed to the lapses in the process of neurulation. The primary neurulation is of prime importance in the development of chick embryo, in which the two sides of flat neural plate begin to converge and involute at the midline and adhere to each other to form the neural tube (Gilbert, 2003). Any failure in this closure towards the rostral and/or caudal end, results in conditions like anencephaly and/or spina bifida respectively and if the tube fails to fuse throughout the body it would lead to rachischisis. The present study reveals such defects in neural tube closure on day 2 in the pesticide treated embryos. Hence, we looked into the molecular regulators of these embryonic events.

The chick embryo expresses E-cadherin and L1-CAM throughout the ectoderm during the neurulation process (Taneyhill, 2016). These Ca^{2+} dependent cell adhesion molecules are the identity of the neuro-ectodermal plate and their expression regulates the fusion process. Due to the switch in gene expression, N-Cadherin comes into picture which marks the separation of ectodermal and non-ectodermal cell types (Taneyhill, 2016). Herein, our results showed downregulation in mRNA expression levels of E-cadherin (*CDH1*), N-cadherin (*CDH2*) and *L1-CAM* in the Ci treated embryos when compared to the control embryos on day 2 and 4. This dysregulation, especially in N-cadherin levels must have led to the improper closure of the neural tube, thereby disturbing the neurulation and causing anomalies in the rostral region of the embryos. Similar results were reported by Detrick and colleagues (1990) wherein deficiency of N-cadherin levels induced morphological defects in *Xenopus* embryos.

Further, as the surface ectoderm separates from the newly formed neural tube, a group of cells delaminate from its anterior most layer, undergo epithelial to mesenchymal transition and migration to further diversify into various cell types termed as cranial neural crest cells. These multipotent cells in the later stages of development give rise to forebrain meninges, craniofacial cartilage, bones of the jaw, neurons and glia in the vertebrate embryo (Meulemans and Bronner-Fraser, 2004; Mayor and Theveneau, 2013). The formation of neural crest cells is a complex process carried out under the influence of micro-environment signals that confer patterning and migratory capabilities to this cell population (Nikolopoulou et al., 2017). Many genes and transcription factors such as SHH, WNTs, BMPs, FGFs and PAX6 are secreted from the adjacent tissues to induce patterning in the neural tube in a gradient fashion (Kulesa et al., 2010; Bragdon et al., 2011; Reid et al., 2011; Prasad et al., 2012; Yardley and García-Castro, 2012; Griffin et al., 2013). Depletion of neural crest cells or perturbations in the gene expressions during patterning process, have been reported in mouse models to cause neural tube defects, microphthalmia and reduced size or absence of jaw structures, suggesting their importance in the development of the future brain (Wilde et al., 2014).

The neural tube undergoes patterning along its two major axes, dorso-ventral (DV) and anterior-posterior (AP), to form a functional nervous system under the activities of paracrine factors secreted from ventral floor plate and dorsal roof plate. SHH cooperates with BMP7, to play an important role in patterning the dorso-ventral axis of the nervous system. Mutations in the SHH gene in mouse and humans have suggested its role to be critical around birth (Ahlgren and Bronner-Fraser, 1999). In addition, targeted deletion of SHH causes significant craniofacial defects such as holoprosencephaly and cyclopia (Xavier et al., 2016). Moreover, knockout studies of BMP7 in mice have clearly indicated its role in the development of eye structures (Solloway and Robertson, 1999). In the present study, the mRNA expression analysis on day 2 and 4 embryos showed a relatively downregulated expressions of *SHH* and *BMP7* in Ci treated embryos, which might have also led to the craniofacial deformities and defects in eye development.

Another important family of signalling molecule, the WNTs is responsible for inducing proliferation in neural tube and thereby regulating multiple aspects of animal development and adult homeostasis (Megason and McMahon, 2002). Salinas (2005) has shown the role of Wnt signals in the vertebrate nervous system for developing axonal guidance to synaptic region. In

the developing vertebrate brain, WNT1, WNT5A and WNT7A are expressed with an overlapping spatiotemporal pattern and any alteration in this signalling pathway leads to cranio-facial dysmorphism (Brault et al., 2001). Also, there are evidences suggesting that the WNTs are acting downstream of the BMPs (Wine-Lee et al., 2004). In the present study, the mRNA expression analysis on day 2 and 4 subjects showed that the Ci treated embryos had a downregulation of *WNT1, WNT5A* and *WNT7A* when compared to the control ones. This dysregulation in their expression might be the consequence of downregulated mRNA levels of *BMP7*, which must have further worsened neural tube development and the cell proliferation. Moreover, neural crest cells are known to be involved in patterning the head and require a synchronized regulation of cell number to tissue size. This probably occurs through a combination of events like cell proliferation and survival which is controlled by SHH (Le Dréau and Martí, 2012; Xavier et al., 2016). It can be hypothesized that diminished levels of *SHH* signalling hampers the growth of the neural tube, primarily because of increased cell death, which leads to an overall reduction in head size in the pesticide intoxicated embryos. We checked the levels of *CASPASE 3* and *PCNA* and found respective hike and fall in their mRNA levels, in treated embryos. The decrease in head size could be an outcome of neural crest cell death and hence, it appears to be its primary determinant. In addition to the defects observed in the present study, we have noted occurrence of wavy neural tube due to intoxication of chlorpyrifos and cypermethrin in combination. This abnormality has been observed in mice with defects in platelet derived growth factor (PDGF) receptor, which is mediated through SHH (Suzuki et al., 2016).

The Sonic Hedgehog, through its downstream GLI zinc-finger transcriptional regulators, orchestrates two major functions; an early patterning and cell proliferation during the neurulation process. However, these factors appear to be absent during migration of cranial neural crest cells (Xavier et al., 2016). Moreover, Aoto and collegues (2002) have documented the involvement of GLI3 in suppressing FGF8 in the developing neural tube of mouse embryo. We have observed similar incidences of *GLI3* downregulation, resulting in the upregulation of *FGF8* expression. Since FGF8 is essential for the control of pattern formation in the developing embryo, its elevated expression can affect the developmental programs of many tissues (Yardley and García-Castro, 2012).

Further, in the embryonic development, the neural tube undergoes drastic changes to attain anterior-posterior identity. Towards the anterior region, the neural tube organizes itself into

three balloon like structures namely the prosencephalon, mesencephalon and the rhombencephalon. These primary vesicles differentiate into secondary structures like forebrain differentiates into telencephalon (forming the cerebral hemispheres) and the diencephalon (forming the optic vesicle for the development of eye), midbrain transforms into mesencephalon and the hindbrain develops metencephalon and myelencephalon (Gilbert, 2003). The boundaries of these vesicles are marked by the presence of SHH and FGF8. Both these paracrine diffusible factors are also involved in patterning of CNC cells in a rostro-caudal manner. Several studies have supported the role of growth factors, including FGF, BMP and WNT as they regulate and define the positional identity of neural crest cells and their derivatives (Suzuki et al., 2016). FGF8, a member of FGF family, is reported to be involved in the neural crest induction, patterning and its migration by upregulating the expression of various transcriptional factors (Yardley and García-Castro, 2012). FGF8 along with SHH marks the midbrain and hindbrain boundary, by silencing the HOX gene expression in the pre-migratory CNC cells (Irving and Mason, 2000). Several lines of evidence have also stated overexpression of FGF8 leading to severe developmental defects in telencephalon, mesencephalon and pharyngeal arches (Martin and Kimelman, 2012; Shao et al., 2015). Cell patterning in the anterior most part of the brain requires low levels of FGF8 for induction of HOX10A and HOX11A which confers positional identity to CNC cells in the brain. In the present study, we observed an elevated expression of *FGF8* which could be a plausible reason behind downregulation of *HOX* genes and therefore, leading to underdeveloped telencephalon in pesticide treated embryos. A study in mice showed heightened FGF8 expression and its activation by WNT in the neural crest cells, which leads to severe craniofacial abnormalities, including exencephaly and anophthalmia (Prakash et al., 2006). Further, the levels of transcription factor PAX6, involved in migration of CNC cells, was fond evaluated. PAX6 is influenced by FGF to mediate morphogenesis of the CNC cell derivatives to form facial structures (Makarenkova et al., 2000). Normal expression of PAX6 is required to guide CNC cells migration for forebrain patterning. In the development of eye, role of PAX6 appears to be of prime importance in the communication between CNC cell derivatives, required for lens induction as well as for corneal and retinal development (Nelms and Labosky, 2010). The downregulated levels of *PAX6* suggests its inefficiency to guide CNC cells to form optic stalk leading to absence of optic cup and causing anophthalmia in the pesticide treated embryos.

As described by Knight and Schilling (2013), neural crest cells are derived from the anterior most part of the neural plate and have the potential to form the skeletal tissue. In avian model

system, little is known about the genetic regulation of cranial vault development. Most of the skeletal system undergoes endochondral ossification, to differentiate mesenchymal cells into chondrocytes, eventually leading to bone formation (Kronenberg, 2003). In the current study we have observed severely compromised chondrogenesis, especially in the craniofacial region of the chicks due to pesticide poisoning. To get insight into the extend of bone and cartilage formed by day 10 chick embryos, head region of control and treated groups were stained with Alcian blue and Alizarin red. The pesticide in question delayed the bone formation in the dosed group as compared to control. The cartilage formed was checked biochemically, by estimation of hydroxyproline. Hydroxyproline is the amino acid found in the highest concentration in collagen. This fibrous structural protein is abundantly seen in cartilage. During early embryogenesis, the skeletal system is made up of cartilage, from mesenchymal tissue, which further differentiates into chondrocytes and later replaced by endochondral ossification. The treated groups showed diminished level of hydroxyproline indicating less amount of cartilage formed as compared to control indicating the toxic manifestation of Ci.

There are ample evidences in the literature proving the role of BMPs in inducing bone formation and regulating chondrogenesis (Kamiya and Mishina, 2011). The use of genetically modified mice has unearthed various signalling pathways activated by BMPs that control multiple aspects of chondrogenesis (Kugler et al., 2015). Herein we have chosen *BMP2* and *BMP7* for the study as they play a major role in chondrogenic and osteogenic differentiation. It was suspected that the Ci treatment might have hampered the BMP signalling and hence, hindered the process of cartilage formation and condensation. In order to test the above notion a mechanistic study, primarily focusing on the expression pattern of *BMP2* and *BMP7* was performed and were found to be significantly downregulated in the pesticide treated embryos. The bone morphogenetic proteins target transcription factors that induce differentiation of mesenchymal cells toward ossification in which SOX9 and RUNX2, are important. SOX9 is a chondrocyte marker expressed during early differentiation stages. Gene expression studies in mouse have been documented, suggesting its role in activating chondrocyte-specific markers such as COL10A1, COL2A1 and Aggrecan to form cartilage (Kelly and Jacobs, 2010; Shen et al., 2010). On the other side, to differentiate chondrocytes into osteoblasts, a member of the runt homology domain factor RUNX2 is required. Also, its expression is suggested to be causing proliferation of osteoblast progenitors and thus regulating the first check point of chondrocyte maturation to osteoblasts (Kelly and Jacobs, 2010; Shen et al., 2010). The analysis of the result showed the toxic manifestations of the combination insecticide by downregulating

mRNA expression levels of *RUNX2, SOX9* and *COL10A1*. This derailment in the signalling pathway must have caused impromptu sculpting of the head and facial structures in the treated embryos.

The cranial vault in the chick embryo forms almost entirely by the endochondral ossification. DLX5, a transcription factor from distal-less homeodomain-containing family, is expressed before osteoblast differentiation as well as in proliferating osteoblast precursors and is required for craniofacial morphogenesis (Holleville et al., 2003). It is mainly expressed during the formation of structural elements such as cartilage. DLX5 null mutations in mice have testified its part in triggering skeletal defects in the form of deferred endochondral ossification and abnormal osteogenesis. Knockout studies have reported craniosynostosis syndromes and severed chondrogenesis (Holleville et al., 2003). Herein, pesticide intoxication led to high levels of DLX5 expression in the treated embryos. Heightened expression of DLX5 impairs differentiation of chondrogenic precursors into osteoblasts of humans (Holleville et al., 2003). *DLX5* transcription in the current study, might have been upregulated by *BMP4* and *BMP7* when expressed together.

Another major factor in skeletal development is the expression of WNTs, which are crucial signals for regulation of chondrocyte and osteoblast differentiation (Day and Yang, 2008). Wnt5a is involved in pattern formation along the AP axis by regulation of chondrogenic differentiation through SOX9. On the contrary, it suppresses hypertrophic chondrocytes by inhibiting RUNX2 expression (Bradley and Drissi, 2010). The pesticide treated embryos showed downregulation of *WNT5A* expression, thereby inhibiting the formation of chondrocytes by significantly suppressing the expression of *SOX9*.

It is well established that BMP2 plays a critical role in osteoblast function mediating its activity through hedgehog signalling. Gli proteins play an essential role as transcriptional activator (GLI2) and repressor (GLI3) in embryonic development by regulating Shh target genes. Null mutation of GLI2 in mice have caused structural defects (Mai et al., 2012). Sonic hedgehog stimulates BMP2 activity in osteoblast differentiation and the effects of SHH are mediated by GLI2 (Zhao et al., 2006). In the present study, we observed reduction in mRNA levels of *SHH* and *GLI2*, affecting further expression of *BMP2* and its downstream effectors. Both the signals together indicate their expression to be a powerful activator of *BMP2* which is imperative for normal osteoblast differentiation. GLI3, a transcriptional repressor of SHH pathway, also has

been reported to trigger skeletal defects in mice and humans (Yip et al., 2019). Downregulated levels of *GLI3* observed in the current study support the concept of *FGF8* overexpression, causing abnormal apoptosis of the skeletal tissues. A similar report wherein defects in GLI3 and FGF8 signalling causing neural tube related defects in mice (Putoux et al., 2018) further consolidates the veracity of the present observation.

The study was further extended to understand the role of FGFs in skeletal development wherein FGF2 and FGF8 are the major candidates. The results vividly expressed that pesticide treatment induced downregulation of *BMP2* and *BMP7*, possibly as a result of the increased expression of *FGF8* which is known to antagonize the action of BMP (Yoon and Lyons, 2004). Moreover, it has been documented that the upregulated expression of FGF8 will activate the apoptotic pathway (Wan and Cao, 2005). To ascertain the extent of cell death, day 10 chick embryos were extracted, and *CASPASE 3* activity was checked. It was observed that *CASPASE 3* activity increased progressively by several times in treated groups compared to the control group animals. Overall it showed an unusual pattern of apoptosis due to diminished BMP signalling in Ci treated group. Kawane and colleagues (2018) have elaborated the role of FGF signalling in skeletal development, craniosynostosis and the progression of some breast cancers. The osteoblast differentiation and proliferation of osteoblast progenitors requires a positive signal from RUNX2 (as discussed earlier) and fibroblast growth factor 2 enhances its ability through MAPK pathway. We found contrary result where *FGF2* mRNA levels showed upregulation however, *RUNX2* mRNA levels remained downregulated in the treated embryos. Similar result was reported by Moore et al., (2002) wherein elevated levels of FGF2 were localised in the undifferentiated mesenchyme around the bones in the chick embryonic tissue. These results suggest that there could be other factors acting upstream of RUNX2 in controlling osteogenesis and chondrogenesis. And conclusively, our observations when monitored at microlevel could be connected to not just isolated signalling molecules but too many of such regulatory molecules, which sets an alarm as to how devastating a toxic exposure during the phase of embryonic development could be.

4.11. CONCLUSION

The pesticide treated embryos showed various congenital malformations in the head region due to aberrant mRNA expressions of the regulatory signals of the cellular processes like cell migration, differentiation, proliferation and survival. We observed defects in the closure of neural tube that form the craniofacial cartilage. Also, incoherent chondrogenesis was noted in

the cranial vault. The development of head is under intricate control of the regulatory signal, rely on constant inter-communication between the morphogens and the surrounding tissues that displayed erroneous results due to pesticide intoxication. Because of the reduced levels of cell adhesion molecules and major regulatory signals like *SHH, BMP7, FGF8*, the neural tube failed to close and morphogenetic movements were affected. In the later development, the neural tube failed to pattern the tissues to form telencephalon along with other brain vesicles. The failure in cell migration process lead to the absence of eye stalk on day 2 which added clues in occurrence of anophthalmia on day 4. The toxic manifestations of the pesticides were later seen in the developing embryos (day 10) where the cranial structures were unsuccessful to differentiate and ossify. These abnormal cranial structures were the derivatives of neural crest cell derived mesenchymal cells that underwent impromptu signalling at early stages. The pesticide dosed embryos thus faced a grave consequence in achieving their cell fate due to the derailment in the expression pattern of the supervisory signals which ultimately led to the craniofacial dysmorphism.

4.12. SUMMARY

Pesticides despite being agents that protect the plants and humans from noxious pests, are infamous for their potential to cause detrimental health issues in nontargeted species. In order to ascertain the latter, a set of experiments were conducted by exposing early chick embryos to a widely used combination insecticide (Ci, 50 % chlorpyrifos and 5 % cypermethrin). The results revealed a myriad of congenital defects pertaining to craniofacial development such as anophthalmia, microphthalmia, exencephaly as well as deformed beak and cranial structures. These teratological manifestations could be attributed to the Ci induced alteration in the titre of major regulators of neurulation and ossification. Therefore, the mRNA and/or the protein level expression pattern of genes which are reported to be involved in the craniofacial development were studied at selected time points of embryonic development. The analysis of the result showed that there have been significant alternations in the expression patterns of the signalling molecules such as *SHH, WNTs, CDH1, CDH2, L1CAM, PAX6, HOX, PCNA, GLI3, BMP7, FGF8, GLI2, SOX9, RUNX2, DLX5, COL10A1, CASPASE 3* etc. on embryonic days 2, 4 and/or 10. Concurrently, on day 10, whole-mount skeletal staining and biochemical estimation of hydroxyproline were carried out in the cranial tissues of the embryos. The overall result of the current study indicates that exposure to Ci during early development impede the crucial regulatory signals (Figure 4.17) that orchestrate the morphogenesis of cranial neural crest cells

thereby hindering the normal progression of neural tube and endochondral ossification which collectively lead to craniofacial dysmorphism in domestic chicks.

Tables

Group	Day 2	Day 4	Day 10
Control	4 (2,6)	4 (3,7)	5 (2,5)
Treated	12(9,13) ***	9 (8,12)***	12 (10,16)***

Table 4.1: Mortality on day 2, day 4 and day 10 for sub-lethal dose Combination insecticide: The values represent mode with range in parenthesis; n=10 with 30 eggs per group per experiment; ***p≤0.001.

Group	Day 2	Day 4	Day 10
Control	0 (0,1)	0 (0,2)	2 (0,2)
Treated	9 (9,13) ***	14 (11,15) ****	12 (10,14) ***

Table 4.2: Malformation on day 2, 4 and 10 from live embryos: The values represent mode with range in parenthesis; n=10 with 30 eggs per group per experiment; ***p≤0.001, ****p≤0.0001.

Protein	Mean ± SEM (arbitrary units)	
	Control	Treated
Day 2		
N-CADHERIN	88.16 ± 8.2	58.23 ± 5.5*
E-CADHERIN	40.25 ± 3.89	27.06 ± 2.4*
SHH	59.11 ± 5.98	27.52 ± 2.9**
PAX6	74.95 ± 7.24	45.91 ± 4.3*
B-ACTIN	96.44 ± 9.1	100.1 ± 10.12
Day 4		
CL.CASPASE3	23.55 ± 2.3	45.89 ± 3.52**
SHH	78.96 ± 7.96	43.26 ± 4.5*
B-ACTIN	114.99 ± 11.2	100 ± 10.1
Day 10		
BMP2	55.32 ± 4.23	27.56 ± 2.5**
SHH	82.88 ± 7.1	60.25 ± 5.23*
B-ACTIN	100 ± 8.3	99.3 ± 8.23

Table 4.3: Spot densitometry analysis of the western blot bands on day 2, 4 and 10 from live embryos. The Values represent Mean ± standard error of mean; n=3 with 30 eggs per group per experiment; *p≤0.05, **p≤0.01.

Group	Day 10 Head Size (mm)
Control	10.692 ± 0.09
Treated	8.372 ± 0.08****

Table 4.4: Morphometric analysis of cranial region of day 10 embryos. The Values represent Mean ± standard error of mean; n=3 with 30 eggs per group per experiment; ****p≤0.001.

Gene	Mean ± SEM
SHH	0.041406 ± 0.003***
CASPASE-3	5.89 ± 0.340***
WNT5A	0.4081 ± 0.014**
FGF8	5.249248 ± 0.039***
WNT7A	0.116231 ± 0.004***
L1CAM	0.155403 ± 0.020***
BMP7	0.335943 ± 0.042***
GLI3	0.301888 ± 0.025***
PCNA	0.533664 ± 0.024*
WNT1	0.406431 ± 0.049**
HOX10A	0.077208 ± 0.006***
PAX6	0.030711 ± 0.002***
HOX11A	0.022543 ± 0.001***
CDH1	0.393014 ± 0.025**
CDH2	0.433156 ± 0.035**

Table 4.5: mRNA expression pattern of the genes involved in regulation of morphogenesis for Ci treated day 2 embryo. Fold change values for control embryo is 1.0 for all the genes (*: $p \leq 0.05$; **: $p \leq 0.01$; ***: $p \leq 0.001$)

Gene	Mean ± SEM
SHH	0.089 ± 0.004***
CASPASE-3	9.415 ± 0.780***
WNT5A	0.126 ± 0.023***
FGF8	6.183 ± 0.048**
WNT7A	0.440 ± 0.029**
L1CAM	0.273 ± 0.030***
BMP7	0.863 ± 0.083
GLI3	0.103 ± 0.001***
PCNA	0.428 ± 0.024**
WNT1	0.073 ± 0.005***
HOX10A	0.006 ± 0.0007***
PAX6	0.197 ± 0.012***
HOX11A	0.013 ± 0.0007***
CDH1	0.140 ± 0.026***
CDH2	0.077 ± 0.009***

Table 4.6: Transcript level expression of genes involved in neural tube patterning in Ci treated day 4 embryos. Fold change values for control embryo is 1.0 for all the genes (*: $p \leq 0.05$; **: $p \leq 0.01$; ***: $p \leq 0.001$)

Gene	Mean ± SEM
SHH	0.176 ± 0.011***
CASPASE-3	4.485 ± 0.320***
WNT5A	0.428 ± 0.031*
FGF8	2.378 ± 0.120***
FGF2	0.568 ± 0.047
BMP2	0.319 ± 0.022**
BMP7	0.276 ± 0.011**
GLI3	0.566 ± 0.038
GLI2	0.572 ± 0.041
SOX9	0.022 ± 0.001***
RUNX2	0.538 ± 0.041*
DLX5	1.301 ± 0.098
COL10A1	0.044 ± 0.003***

Table 4.7: Transcript levels of genes regulating chondrogenesis in Ci treated day 10 embryos. Fold change values for control embryo is 1.0 for all the genes (*: $p \leq 0.05$; **: $p \leq 0.01$; ***: $p \leq 0.001$)

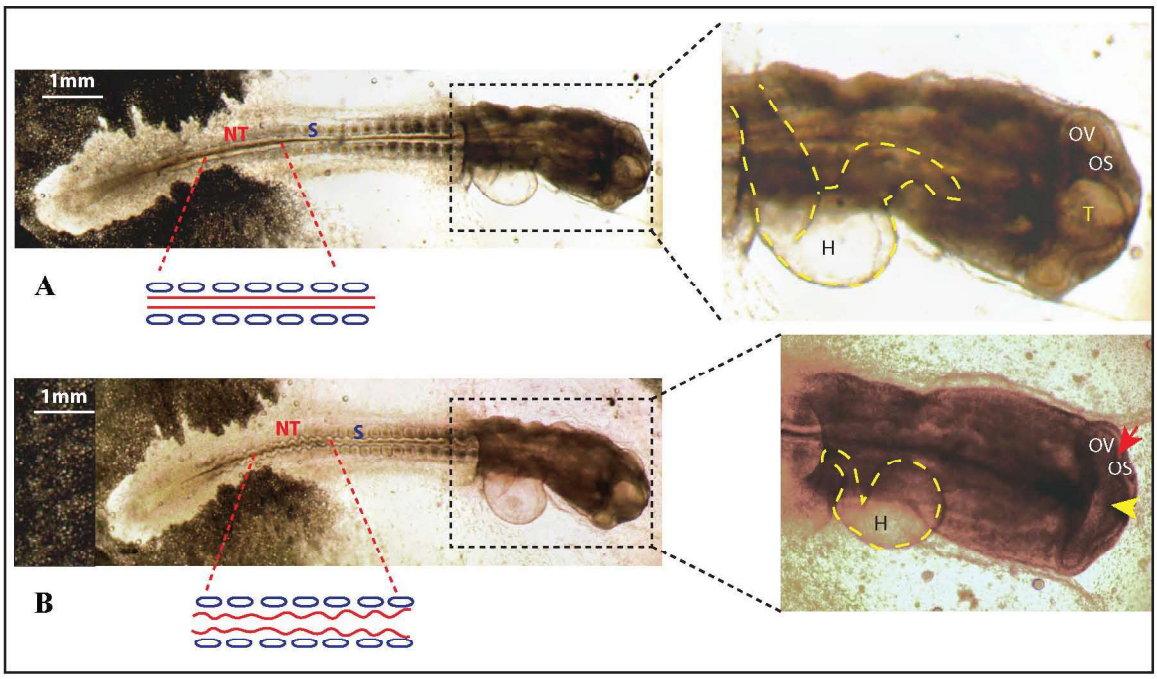

Figure 4.4: Pesticide induced structural defects: (A) Control embryo of day 2 with well-developed S-shaped Heart (H), Neural tube (NT), Optic Stalk (OS), Optic Vesicles (OV), Somites (S) and Telencephalon (T); (B) Ci treated day 2 embryo with under developed Optic stalk (red arrowhead), Telencephalon (yellow arrowhead), irregular heart shape (yellow dotted line) and wavy neural tube (NT)

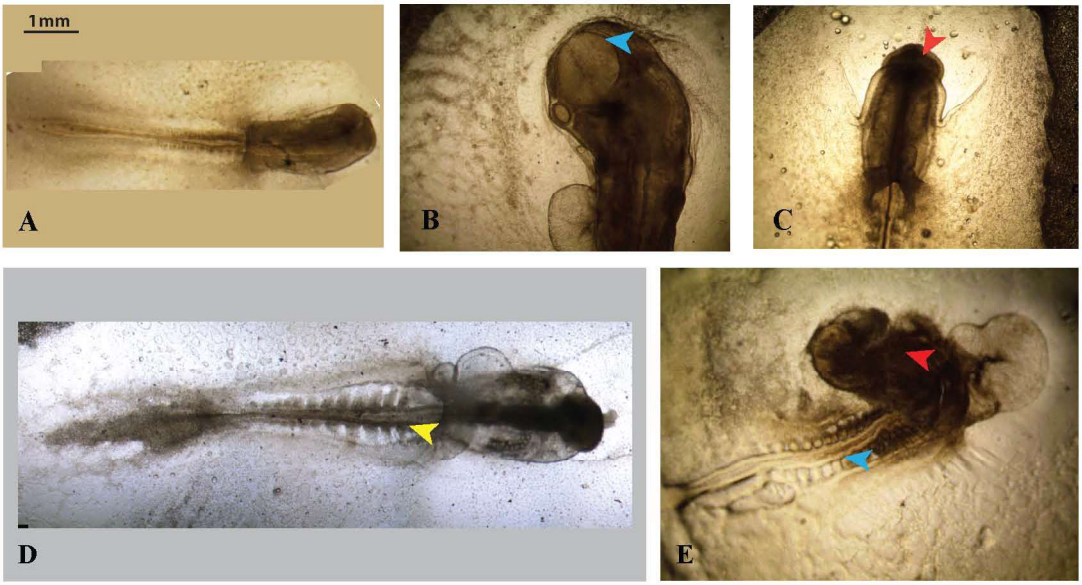

Figure 4.5: Pesticide induced structural defects: (A) Ci treated day 2 embryo showing reduction in size; (B) Absence of eye stalk marked by blue arrowhead in Ci treated embryo; (C) Underdeveloped telencephalon in treated embryo (red arrow head); (D) Defect in closure of neural tube marked by yellow arrow head; (E) Distorted cephalization and deformed neural tube shown by red and blue arrowhead respectively (Scale= 1mm).

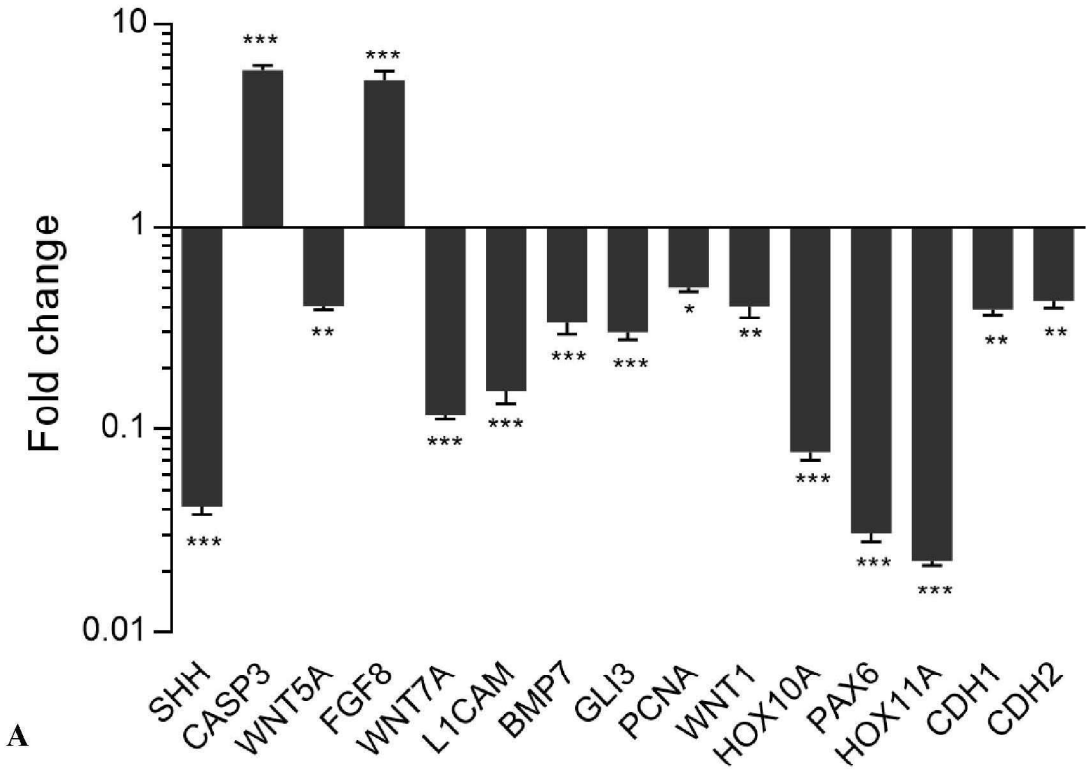

Figure 4.6: mRNA expression pattern of the genes involved in regulation of morphogenesis for Ci treated day 2 embryo. Values are expressed in fold change (Mean ± SEM). Fold change values for control embryo is 1.0 for all the genes (*: $p \leq 0.05$; **: $p \leq 0.01$; ***: $p \leq 0.001$)

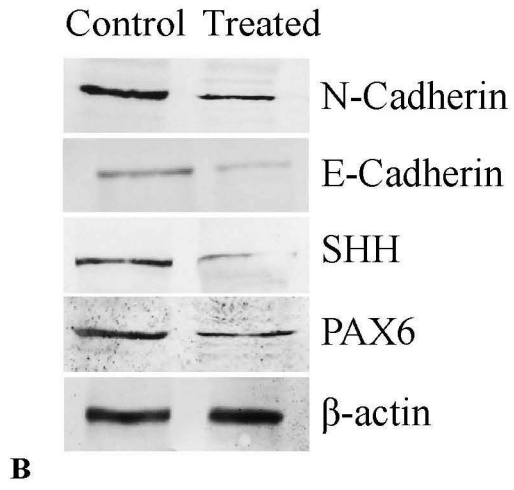

Figure 4.7: Western Blot image showing comparative expression of various proteins: E-Cadherin, N-Cadherin, SHH, PAX6 on day 2. β-actin was taken as loading control, n=10 eggs/group.

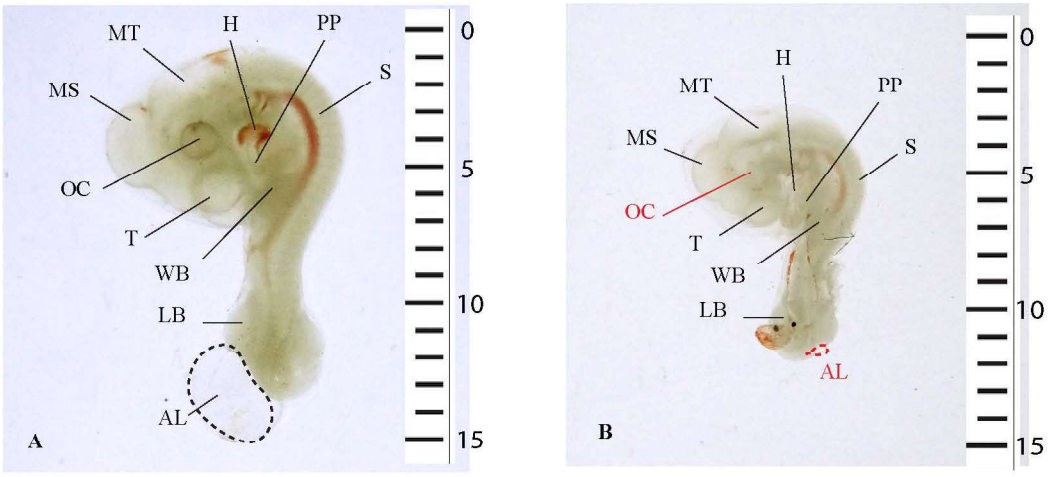

Figure 4.8: Photograph of (A) day 4 Control embryo with well-developed structures indicating Allantois (AL), Leg bud (LB), Mesencephalon (MS), Metencephalon (MT), Optic cup (OC), Pharyngeal pouch (PP), Somites (S), Telencephalon (T) and Wing bud (WB); B) day 4 Treated embryo with reduced allantois and absence of optic cup (marked by red coloured text). Scale in mm

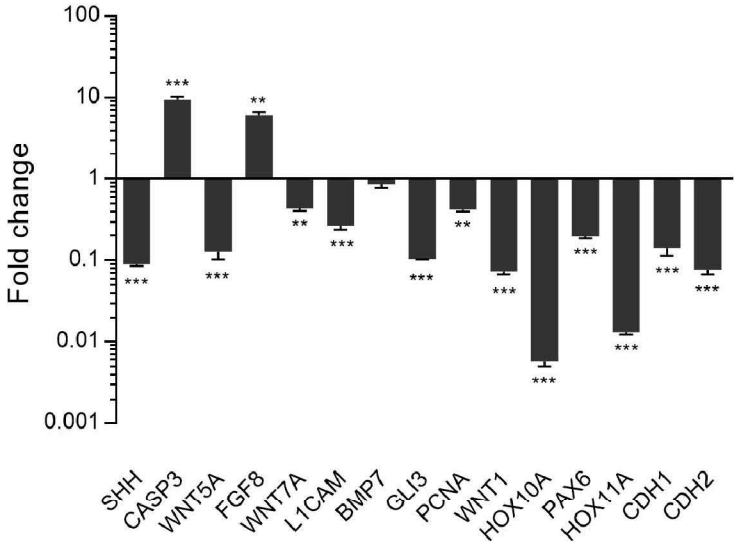

Figure 4.9: Transcript level expression of genes involved in neural tube patterning in Ci treated day 4 embryos. Values are expressed in fold change (Mean ± SEM). Fold change values for control embryo is 1.0 for all the genes (**: p≤0.01; ***: p≤0.001).

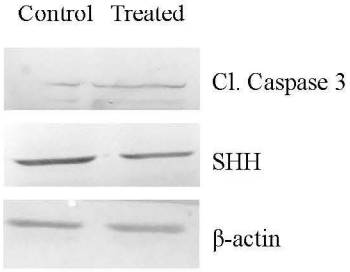

Figure 4.10: Western Blot images showing comparative expression of cleaved CASPASE 3 and SHH on day 4. β-actin was taken as loading control, n=10 eggs/group.

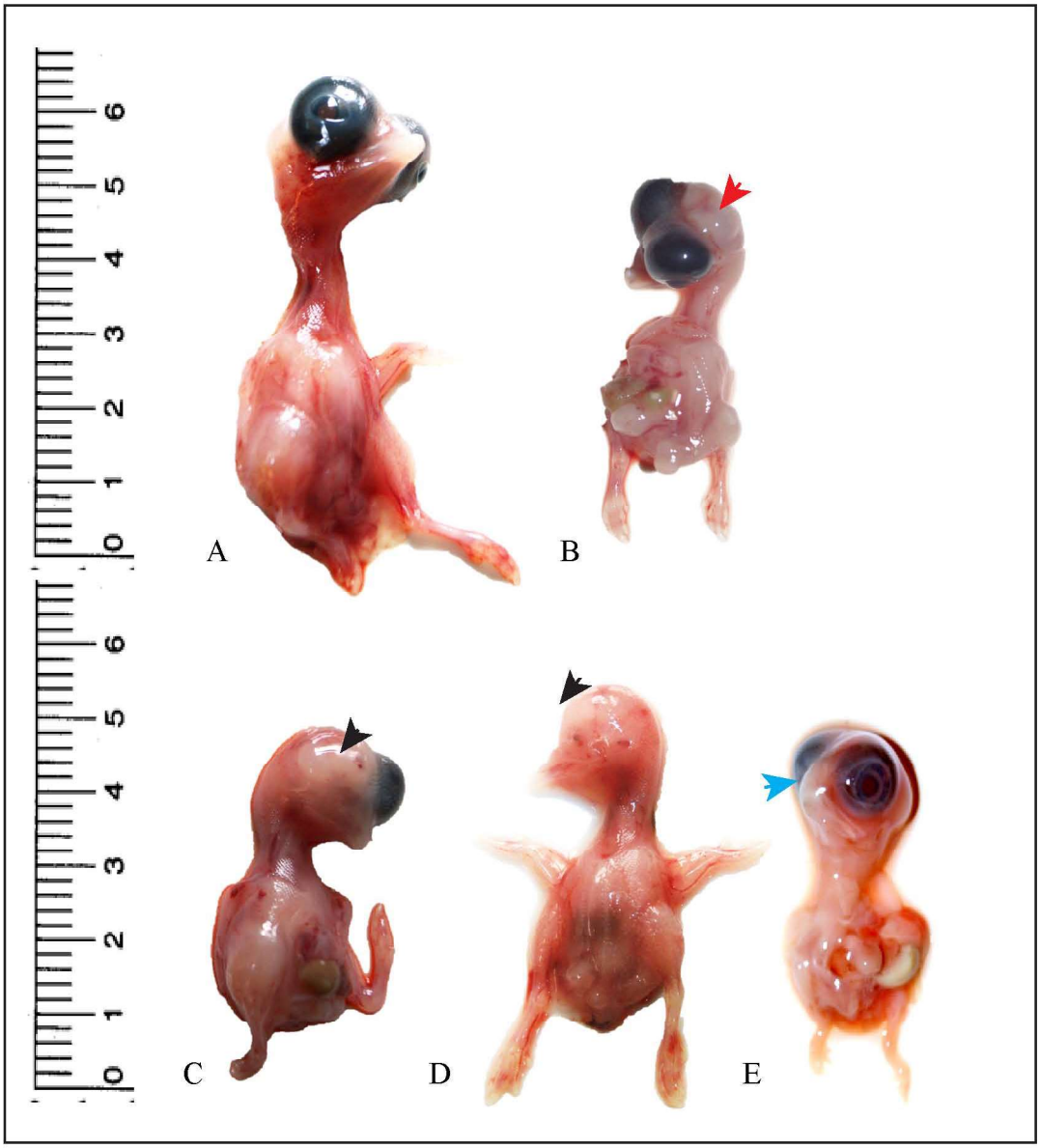

Figure 4.11: Photograph of day 10 Control embryo with well-developed cranio-facial structure (A); Treated embryo indicating exposed brain marked by red arrowhead (B), phocomelia and unilateral anophthalmia (C), Bilateral anophthalmia marked by black arrowhead (D) and beak deformity (absence of beak) shown by blue arrowhead (E) Scale in cm.

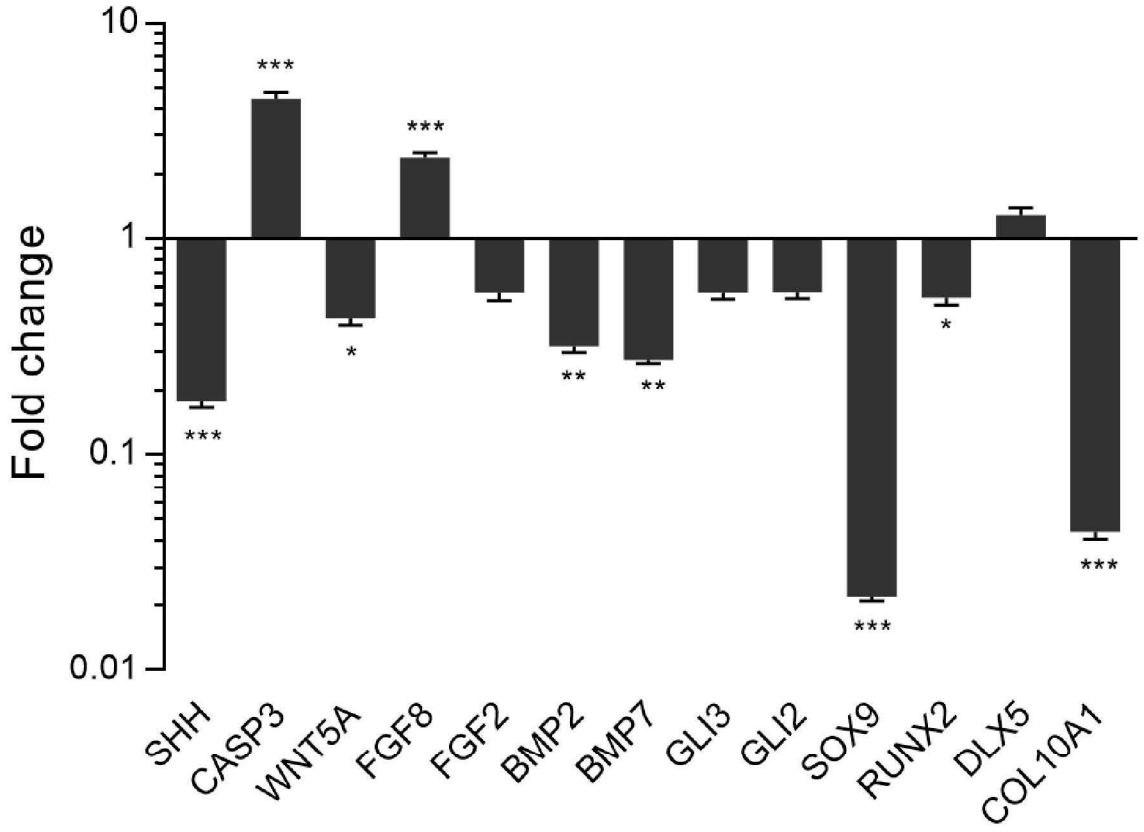

Figure 4.12: mRNA expression pattern of the genes involved in regulation of morphogenesis for Ci treated day 10 embryo. Values are expressed in fold change (Mean ± SEM). Fold change values for control embryo is 1.0 for all the genes (*: $p \leq 0.05$; **: $p \leq 0.01$; ***: $p \leq 0.001$)

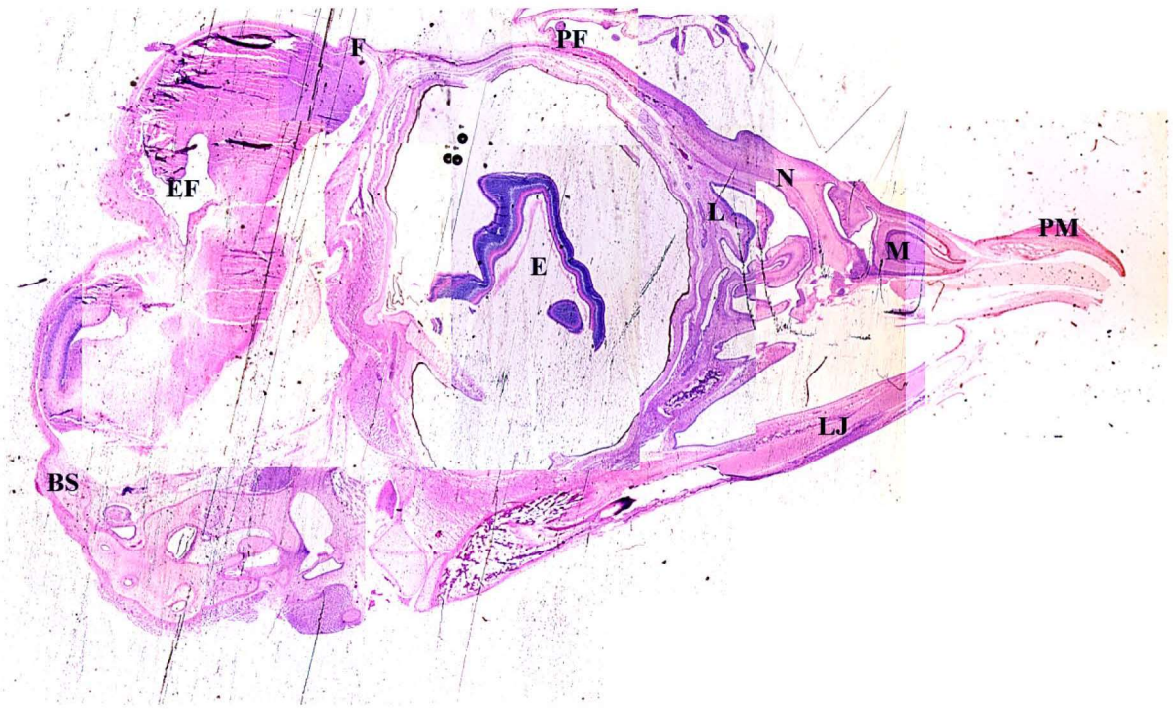

Figure 4.13: Composite image of cross section of day 10 chick embryo from control group showing well-developed cranial region. Where, BS: Base of skull, E: Eye, EF: Ear fossa, F: Frontal, L: Lachrymal, LJ: Lower jaw, M: Maxilla, N: Nasal, PF: Prefrontal, PM: Premaxilla.

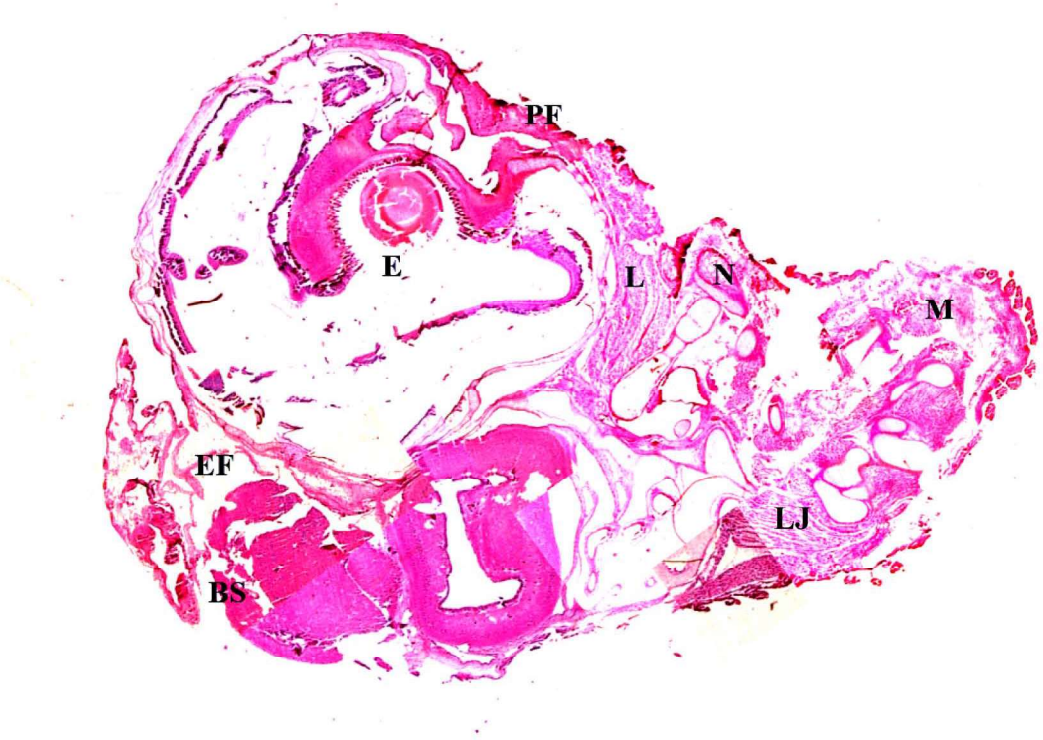

Figure 4.14: Composite image of cross section of day 10 treated chick embryo showing deformities in the cranial region. Where, BS: Base of skull, E: Eye, EF: Ear fossa, L: Lachrymal, LJ: Lower jaw, M: Maxilla, N: Nasal, PF: prefrontal.

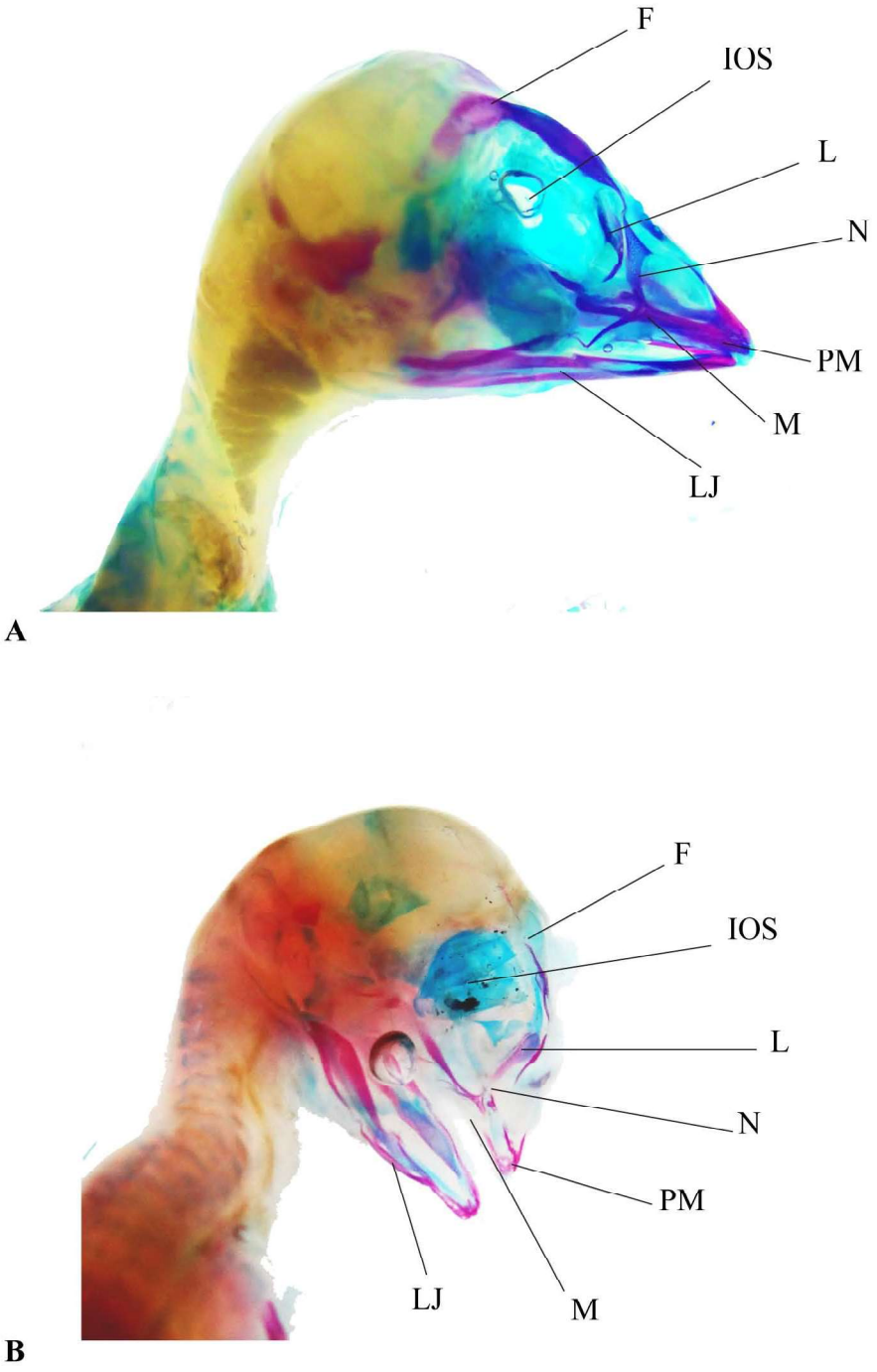

Figure 4.15: Embryos demonstrating differential staining of bone and cartilage in day 10 control (A) and treated (B) embryos respectively (F: Frontal, IOS: Interorbital septum, L: Lachrymal, LJ: Lower jaw, M: Maxilla, N: Nasal, PM: Premaxilla)

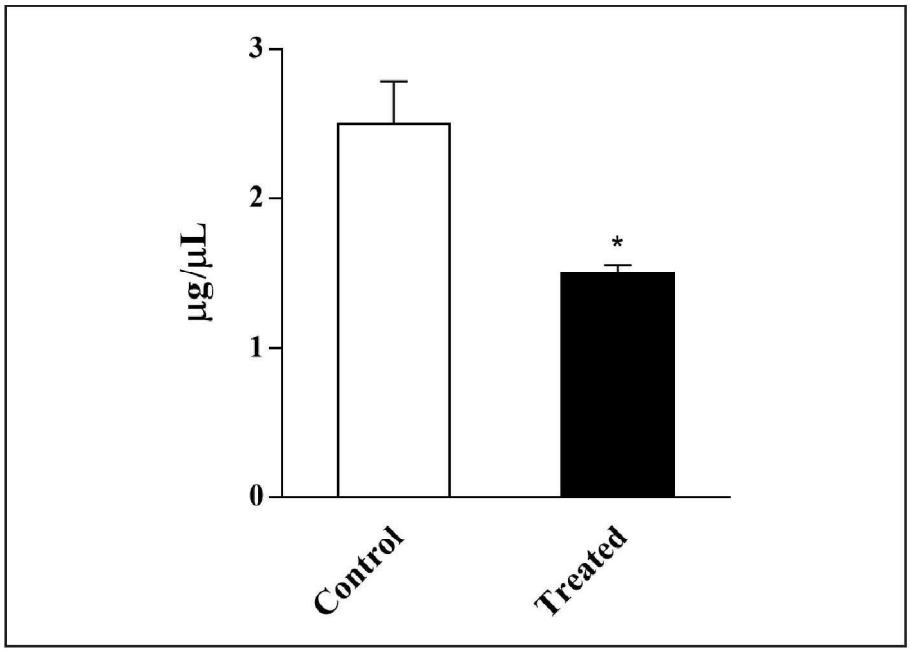

Figure 4.16: Hydroxyproline content in day 10 control and treatment groups n=10 eggs/group (*: $p \leq 0.05$)

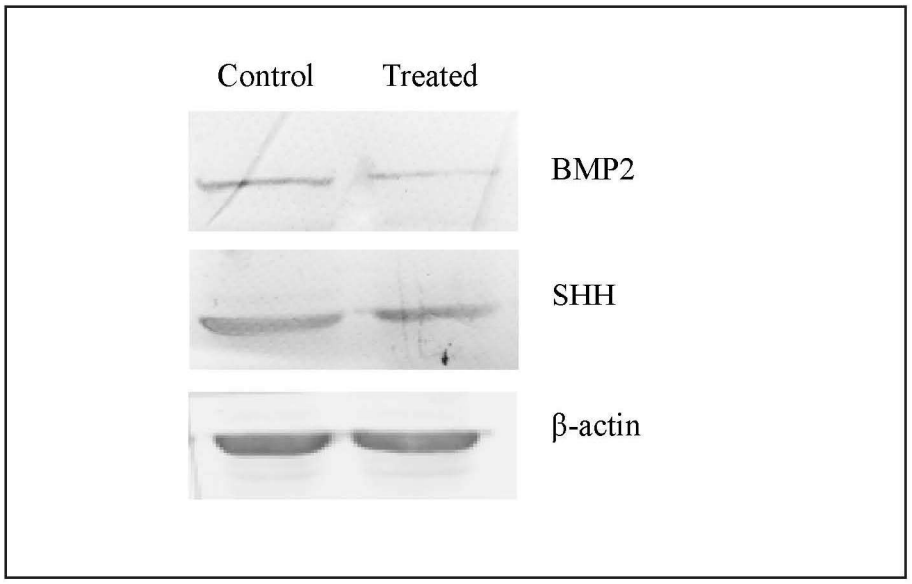

Figure 4.17: Western Blot images showing comparative expression of BMP2 and SHH on day 10. β-actin was taken as loading control, n=10 eggs/group.

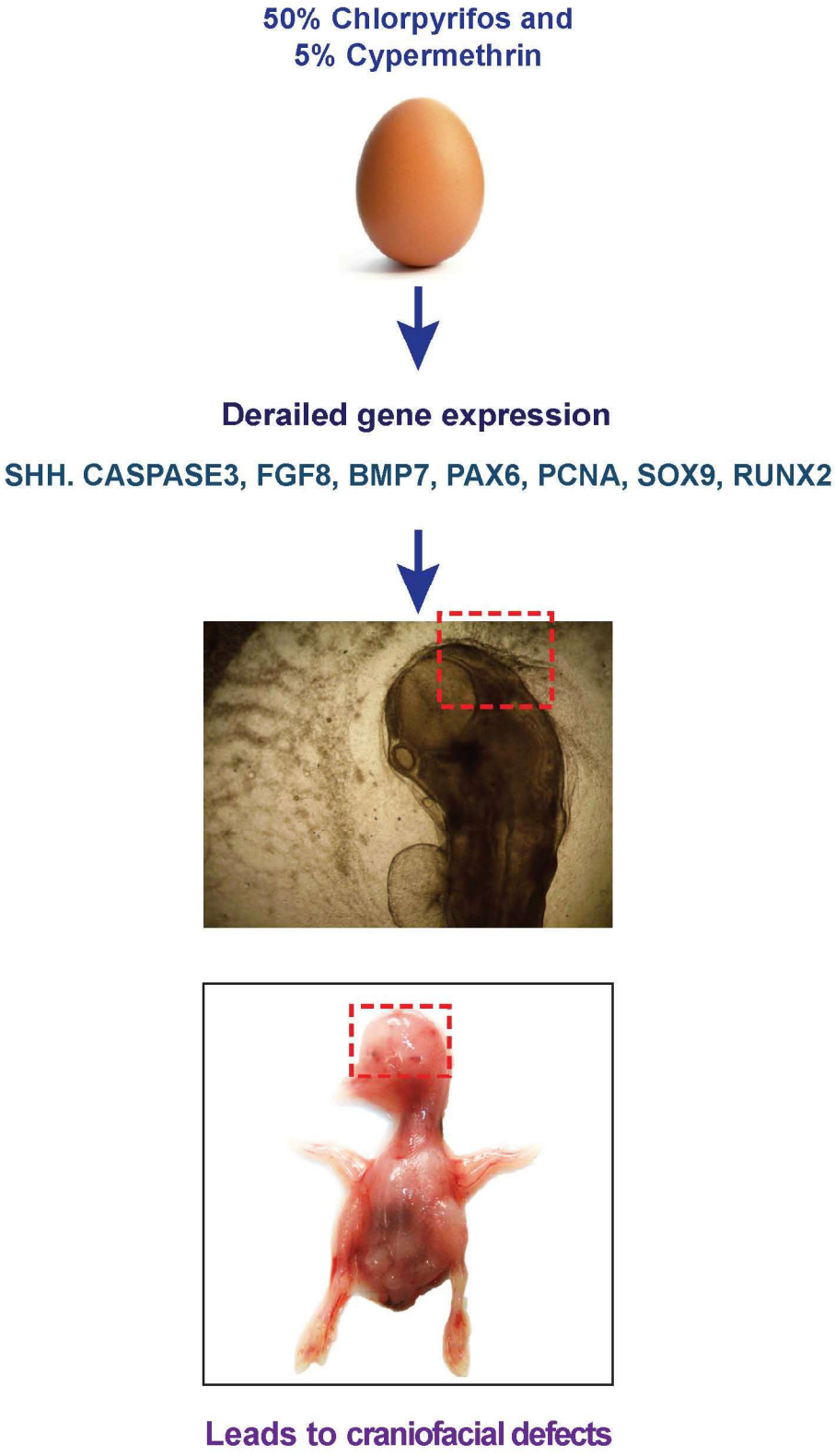

Figure 4.18: Graphical summary displaying effect of Ci in neural tube formation and patterning culminating into craniofacial defects in developing chick embryo